EDGE ARTICLE

Check for updates

Modular synthesis of aryl amines from 3-alkynyl-2-pyrones†

Kristen E. Gardner, [ID] [a] Louis de Lescure,[b] Melissa A. Hardy, [ID] [c] Jin Tan,[a] Matthew S. Sigman,*[c] Robert S. Paton [ID] *[b] and Richmond Sarpong [ID] *[a]

The synthesis of aryl amines from 3-alkynyl-2-pyrones and various amines is described. Mechanistically, the aryl amines are proposed to arise from the 3-alkynyl-2-pyrone substrates through their selective opening in a 1,6-fashion by secondary amines followed by decarboxylation and an unexpected rearrangement. The proposed mechanism is supported by quantum chemical transition-state calculations, which are consistent with the regiochemical outcome. The scope of this transformation spans a variety of 3-alkynyl-2-pyrones and a range of secondary amines. The influence of the secondary amine coupling partners on reaction efficiency was elucidated through data-driven modeling as well as scope exploration. These latter studies revealed that the steric bulk of the secondary amine coupling partner under the reaction conditions serves as a strong indicator of overall reaction efficiency.

Introduction

Methods for fragment coupling (*i.e.*, bringing together two reactive addends), especially in a convergent fashion, are highly valuable for the efficient preparation of complex organic molecules.[1] In particular, metal-catalyzed cross-coupling reactions to form carbon–carbon or carbon–heteroatom bonds have become robust tools for fragment couplings.[2,3] Palladium-catalyzed cross-coupling reactions are powerful tools for this purpose and continue to be widely used in both academia and industry.[4] Because aryl amines feature prominently in agrochemicals,[5] pharmaceuticals[6,7] (see Scheme 1A), natural products,[8,9] and organic molecules of relevance to materials science,[10–12] methods for the robust and facile synthesis of C(sp²)–N bonds (*e.g.*, Buchwald–Hartwig amination reactions[13] or nucleophilic aromatic substitution[14]) are of fundamental importance in organic synthesis. In this Article, we report an alternative approach to prepare aryl amines using 3-alkynyl-2-pyrones. This transformation presents a complement to established approaches for C(sp²)–N bond formation to form aryl amines.

The versatility of 2-pyrones (**1**, Scheme 1B) as starting materials in ring-forming processes has been explored for almost a century.[15] Direct pericyclic annulations of 2-pyrones,
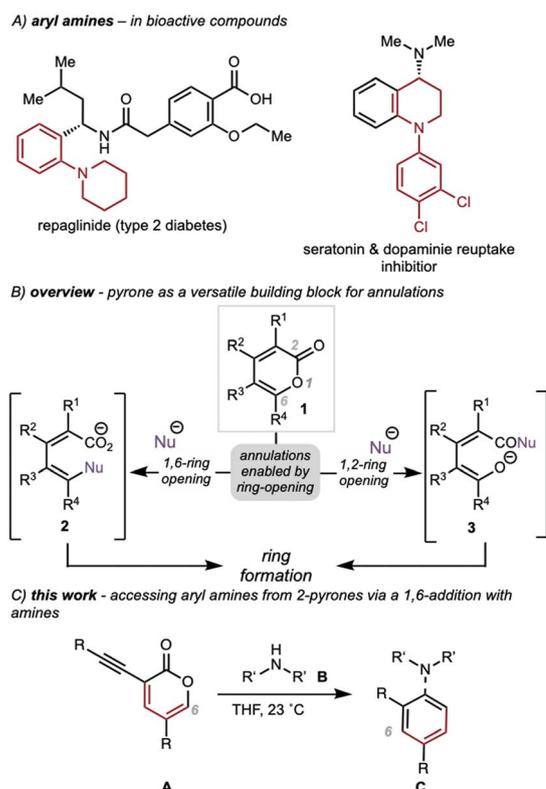
[a]Department of Chemistry, University of California, Berkeley, CA, USA, 94708. E-mail: rsarpong@berkeley.edu

[b]Department of Chemistry, Colorado State University, Fort Collins, CO 80523, USA. E-mail: rpaton@colostate.edu

[c]Department of Chemistry, University of Utah, Salt Lake City, Utah 84112, USA. E-mail: sigman@chem.utah.edu

† Electronic supplementary information (ESI) available. CCDC 2339055. For ESI and crystallographic data in CIF or other electronic format see DOI: https://doi.org/10.1039/d4sc04885g

Scheme 1 (A) Biologically active molecules containing the aryl amine motif. (B) Overview of annulations enabled by the versatility of 2-pyrones. (C) This work: access to aryl amines from 3-alkynyl 2-pyrones.
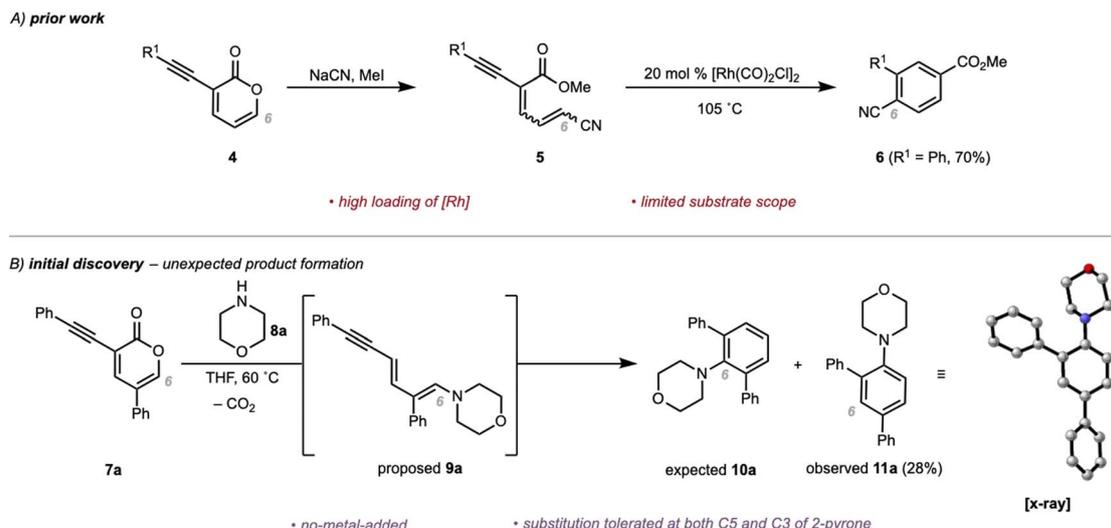
Scheme 2 (A) Prior work of Rh-mediated cyclization to substituted benzoates. (B) Initial discovery of unexpected formation of rearranged product **11a** with no-metal-added.

such as [4 + 2] cycloadditions[16] and 4π electrocyclizations,[17] have proven to be effective tactics for accessing synthetically versatile bicycles. Previously, we developed novel annulation reactions enabled by the nucleophilic 1,6-[18,19] or 1,2-[20] openings of 2-pyrones to access diverse ring systems using, for example, intermediates **2** or **3**. Our ongoing efforts in this area have focused on expanding the scope of this versatile pyrone remodeling strategy to build other scaffolds.

Recently, we reported the synthesis of substituted benzoates from 2-pyrones by exploiting a metal-mediated Hopf cyclization of dienyne adducts accessed from a 1,6-opening of 3-alkynyl-2-pyrones with NaCN (Scheme 2A).[21] Mechanistically, we proposed that nucleophilic attack on a 3-alkynyl-2-pyrone (**4**) in a 1,6-fashion with NaCN followed by trapping of the resulting carboxylate with MeI yields a 1,3-dien-5-yne (**5**). Intermediates such as **5** are then further elaborated to substituted benzoates (**6**) facilitated by Rh-catalysis. However, the scope was limited to aryl groups on the alkyne (R^1 = Ar, Scheme 2A) and the transformation was intolerant of substitution at C5 of the pyrone substrate. On the basis of the proposed mechanism, we hypothesized that the electron-withdrawing nitrile group in **5** was responsible for the poor reactivity of various substrates. We postulated that introduction of a more electron-releasing group (*i.e.*, an amine group; see **8a**) would increase reaction efficiency and broaden the substrate scope.

To test this proposal, 3-alkynyl-2-pyrone **7a** was subjected to morpholine (**8a**), an electron-rich secondary amine. Previously, en route to our total synthesis of delavatine A,[18] we observed spontaneous decarboxylation when substituted pyrones engaged with morpholine in a 1,6-opening. On that basis, we predicted that upon reaction of **7a** and **8a**, spontaneous decarboxylation would occur to form **9a**. Subjection of **9a** to metal catalysis (analogous to our observation for **5** → **6**) was then expected to lead to **10a**. To our surprise, we directly isolated an unexpected constitutional isomer, aryl amine (**11a**), in 28% yield (confirmed by X-ray crystallographic analysis of a single

crystal). The observed isomer implied that the morpholine unit had migrated to a different position following its initial addition in a 1,6-fashion. Overall, this transformation serves as a complement to the Buchwald–Hartwig amination reaction (and other C(sp^2)–N cross-couplings such as Ullman-type couplings) to access aryl amines.[22–26] We studied this transformation in detail in order to explore the substrate scope and gain a mechanistic understanding of this process.

Results and discussion

With the discovery of this "no-metal-added" synthesis of aryl amines from 3-alkynyl-2-pyrones, we first sought to optimize the initial hit (Table 1, entry 1). Decreasing the concentration of the

Table 1 Optimization table with alkynyl 2-pyrone (**7a**). All reactions run on 5.0 mg scale unless otherwise noted

Entry	Equiv. **8a**	Solvent	Temp.	Additive	Yield^a
1	1.5	THF (0.05 M)	60 °C	—	28%
2	2	THF (0.025 M)	60 °C	—	38%
3	2	THF (0.025 M)	23 °C	—	61%
4	5	THF (0.025 M)	23 °C	—	62%
5	2	THF (0.025 M)	23 °C	10 mol% PPh$_3$	55%
6	2	THF (0.025 M)	23 °C	10 mol% acetic acid	45%
7	2	THF (0.025 M)	23 °C	10 mol% NEt$_3$	54%
8	2	THF (0.025 M)	23 °C	No celite filtration	74%^{b}
9	2	THF (0.025 M)	23 °C	No celite filtration	52%^{c}

^{a} Isolated yields. ^{b} Reaction run on 0.05 mmol scale. ^{c} Reaction run on 1 mmol scale under air.

reaction from 0.05 M to 0.025 M, which was expected to inhibit undesired intermolecular reactions to favor the desired intramolecular cyclization, led to a slight increase in yield (entry 2). We found that lowering the reaction temperature to room temperature (23 °C) led to a significant increase in yield (entry 3). We observed that using a large excess of morpholine (**8a**, 5 equiv.) led to no improvement in yield (entry 4). Several additives were evaluated. For example, addition of PPh₃ to aid in *E/Z* isomerization of the ring opened intermediate arising from 1,6-addition (entry 5), acid to aid in proton transfers (entry 6), or base to increase nucleophilicity of **8a** (entry 7) did not improve the reaction efficiency. Modifying the workup to circumvent the poor solubility of the tri-aryl product (**11a**) by direct concentration of the reaction mixture (see the ESI† for more details) led to a significant increase in the isolated yield of **11a** to 74% yield (entry 8). On a 1 mmol scale, **11a** was isolated in 52% yield.

Using these conditions, we investigated the scope of this operationally simple transformation. We began by varying the substituents on the 3-alkynyl-2-pyrone coupling partner (Scheme 3). Alkynyl-pyrone substrates with varied substitution patterns were readily synthesized in two-steps from 3,5-dibromopyrone through Suzuki cross-coupling of various boronic acids to install a substituent at C5,[19,27] followed by Sonogashira cross-couplings of various acetylenes to install the alkyne units at C3.[28] A variety of substrates featuring various groups at the alkyne terminus, including electron-donating (see **11d**) and electron-withdrawing (see **11c** and **11e**) groups were tolerated in

this reaction. Additionally, for non-aromatic alkynyl substituents (*e.g.*, **11g**), the desired product was obtained even at room temperature, albeit in lower yields compared to substrates featuring aryl groups at the alkyne terminus. We also found that a variety of 3-alkynyl-2-pyrone precursors bearing varied substituents at C5 including electron-withdrawing (see **11j**), electron-donating (see **11n**), and heterocyclic (see **11l**) groups performed reasonably well in the transformation. However, when 3-phenyl-alkynyl-5-bromo-2-pyrone was subjected to the reaction conditions, we observed trace product (see **11k**) as well as some of the bis-morpholine adduct. Finally, with a non-aromatic substituent at C5, we observed poor yields of the anticipated product (see **11m**).[29]

To investigate the scope of secondary amine coupling partners, we evaluated a variety of cyclic secondary amines (**8a** to **8o**, Scheme 4A), which were generally well tolerated in this reaction, except in cases where there is increased steric bulk around the nitrogen atom (*e.g.*, **8j**, **8k**, and **8m**). Several acyclic amines (**8p**, **8q**, **8r**, **8s**, **8t**), which are inherently less rigid, were effective coupling partners, albeit leading to the products in somewhat reduced yields than had been achieved using cyclic amines. However, for acyclic α-branched amines (see amines **8u** and **8v**), as well as for bis(methoxyethyl)amine (**8w**), we observed no reactivity and only recovered starting material. Not surprisingly, using non-nucleophilic amines such as *N*-methyl aniline and indole did not result in any observed reaction.[30]
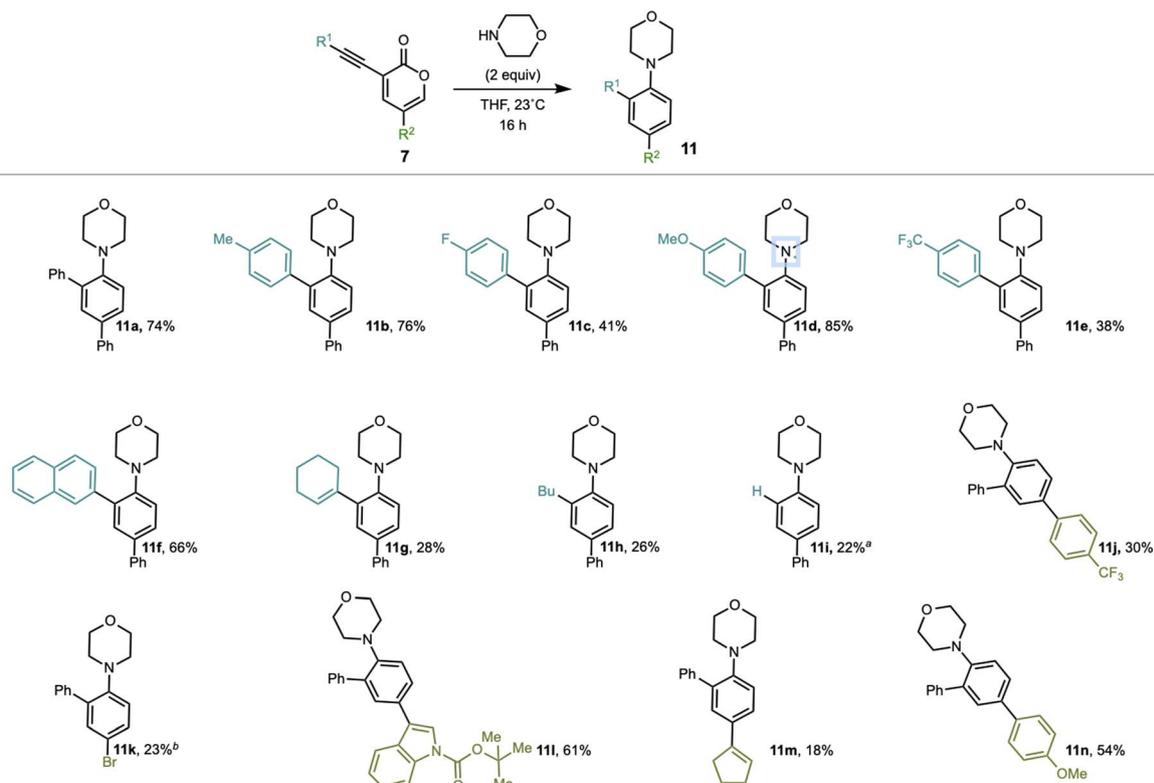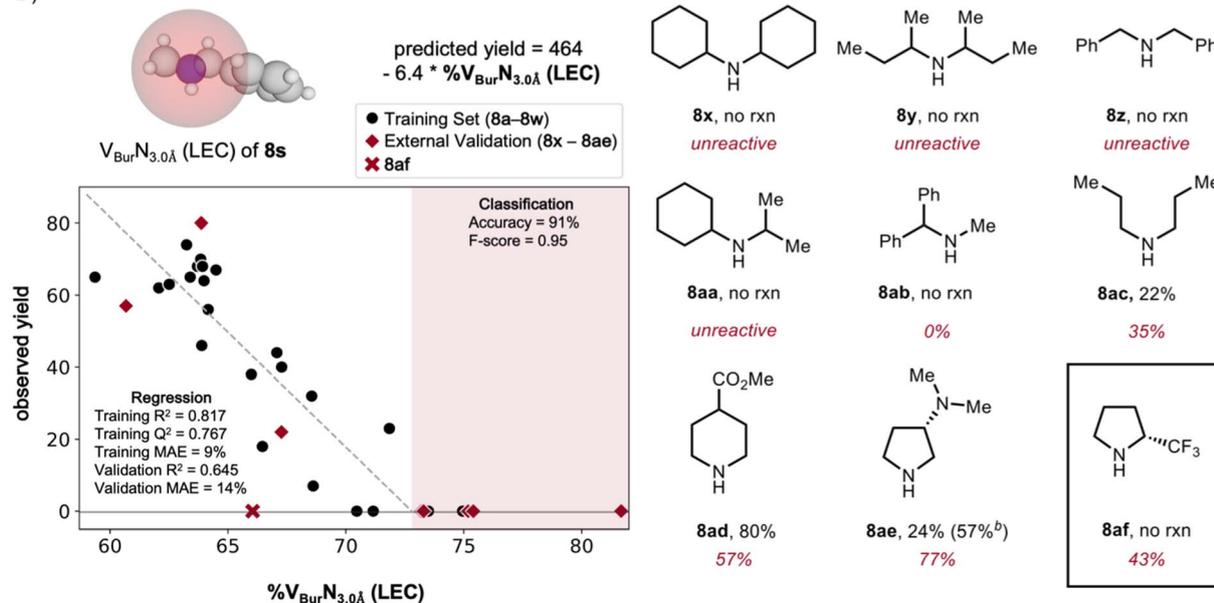

Scheme 3 Substrate scope of alkynyl 2-pyrone. [a]R₁ was TMS. [b]Also isolated 2% of bis-morpholine product.
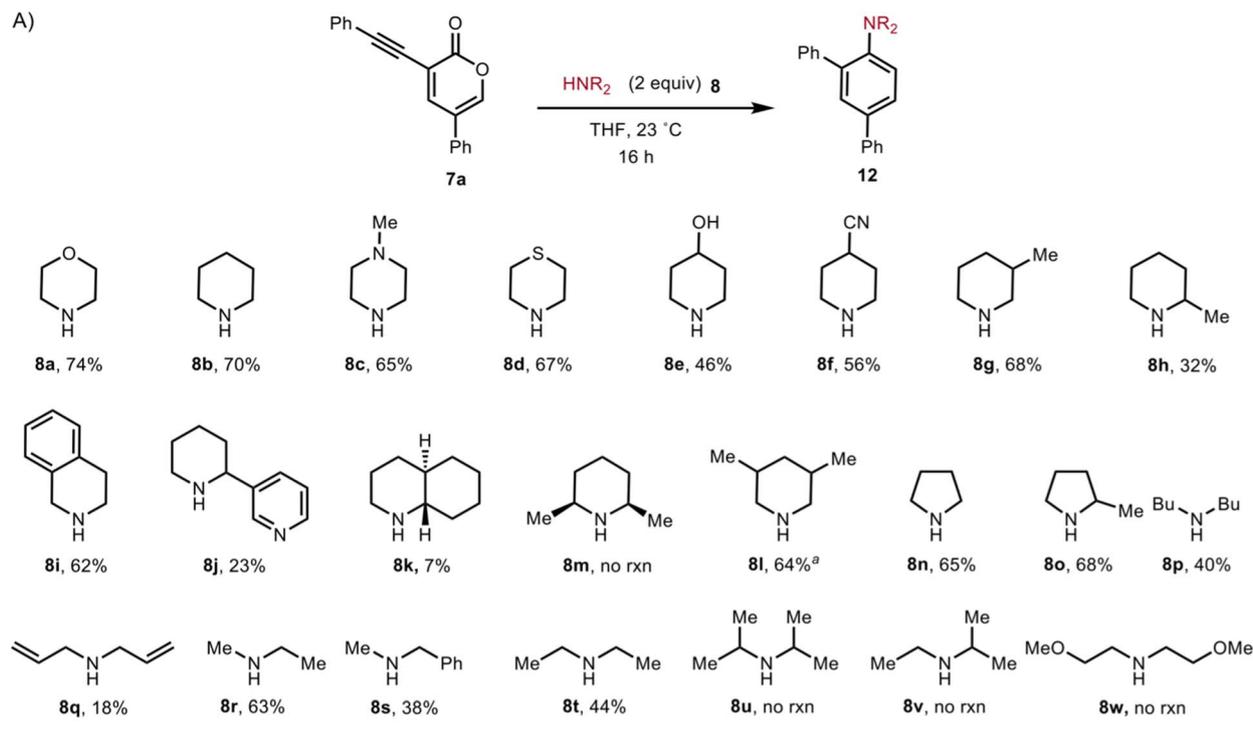
Scheme 4 (A) Substrate Scope of amine. [a]1 : 2 mix *cis/trans* (from amine starting material) [b]NMR yield. (B) Single parameter classification and regression model tested using the selected external validation substrates (right). Observed yields are in black with predicted yields italicized in red. Validation statistics are presented excluding compound **8af**.

To quantify the observed steric effect of the amine coupling partner, we compared the yield of the coupling products (*i.e.*, aryl amines) to molecular descriptors of the corresponding amine. Yield can be a particularly challenging output to model as it is sensitive to multiple factors that are often unique from the intended pathway (*e.g.*, side reactions, isolation, *etc.*).[31] Modeling is additionally complicated at the bounds of yield (0% and 100%) where the relationship becomes non-linear.[30] To

address these challenges, we employed a classification algorithm[32] based on calculated amine descriptors to bin results where productive reaction did not occur. Amine reactivity was classified as "reactive" and "unreactive" regions based on whether the $\%V_{Bur}N_{3.0Å}$ was less than or greater than 73% (Scheme 4B). These steric descriptors were obtained for the lowest energy amine conformer structures optimized in the gas phase at the B3LYP-GD3BJ/6-31G(d,p) level of theory with single

point energies determined at the M062X/def2-TZVP level of theory. Validation substrates were selected from the inactive region to probe the robustness of this threshold (**8x**, **8y**, **8z**, and **8aa**) with the %$V_{Bur}N_{3.0\text{Å}}$ ranging from 73 to 82%. Consistent with the classification model, each of these coupling partners did not react, providing support for the robustness of this threshold with respect to false negatives.

At this stage, linear regression algorithms appeared well-suited to model the "reactive" substrates. The best performing model as given by the training statistics (*i.e.*, R^2, Q^2, and mean average error (MAE)) relied on the same %$V_{Bur}N_{3.0\text{Å}}$ descriptor used for classification, indicating that in general sterically less-congested amines produce higher yields. Five additional amines (**8ab**, **8ac**, **8ad**, **8ae**, and **8af**) were selected to validate the predictive power of the linear regression model, spanning the range of buried volumes previously tested (60% to 73%). While the experimental yields were typically in reasonable agreement with the predicted yield (±20%), the poorest prediction was for amine **8af**, which was predicted to give 43% yield but was found, empirically, to be unreactive. Of note, this compound contains an electron-withdrawing group that is not present in our training data. It is therefore not surprising that this poorly nucleophilic amine (by virtue of the inductively withdrawing CF$_3$ group) is outside the domain of applicability of the model. When amine **8af** was excluded, the validation statistics were comparable to the training set, indicating that while this model is not particularly precise, it offers simple and interpretable insight into the effect of the amine. We hypothesized that the steric bulk of the amine could affect either the addition of the amine to the pyrone, or the rearrangement of the amine-pyrone

adduct (*i.e.*, **Int-I**, Fig. 1) to the corresponding aryl amine, prompting us to undertake further mechanistic studies.

Specifically, we investigated the reaction of **7a** and morpholine, evaluating potential reaction mechanisms with density functional theory (DFT). All structures were optimized at the ωB97X-D/6-31+G(d,p) level of theory, followed by ωB97X-D/def2-TZVP single point energy evaluation. All calculations include an implicit SMD (solvation model based on density) description of tetrahydrofuran. Full computational details are described in the ESI.† We computed a reaction pathway that begins with the irreversible addition of morpholine to the C6 position of pyrone **7a** *via* **TS-I** (Fig. 1), resulting in **Int-I** with an associated barrier of 17.7 kcal mol^{-1}. Of the two positions on the pyrone that will lead to productive reactivity (*i.e.*, C4 and C6) the C6 position is more electrophilic based on NPA-computed atomic charges (0.21 for C6 *vs.* −0.10 for C4). At this stage, we first calculated a pathway where ring opening and decarboxylation lead to dienyne **Int-V-A-Allene** which can then undergo ring closure to cyclic allene **Int-VI-Allene** (see Fig. S8† for details). However, the activation energy of this process was found to be 39.1 kcal mol^{-1} (*via* **TS-VI-Allene**) making it an unlikely route towards the product.

In contrast, our calculations revealed that the addition of a second equivalent of amine nucleophile at C2 of the allene is both kinetically and thermodynamically feasible and provides access to an intermediate for which ring-opening is much more facile. This pathway first involves exergonic tautomerization to an allene (**Int-II**, $\Delta G = -2.3$ kcal mol^{-1}). The cis configuration of the amine relative to the allene is slightly more stable than the trans diastereomer. Nucleophilic addition of a second equivalent of morpholine, now to **Int-II** (*via* **TS-III**, $\Delta G^{\ddagger} = 16.4$ kcal mol^{-1}) leads
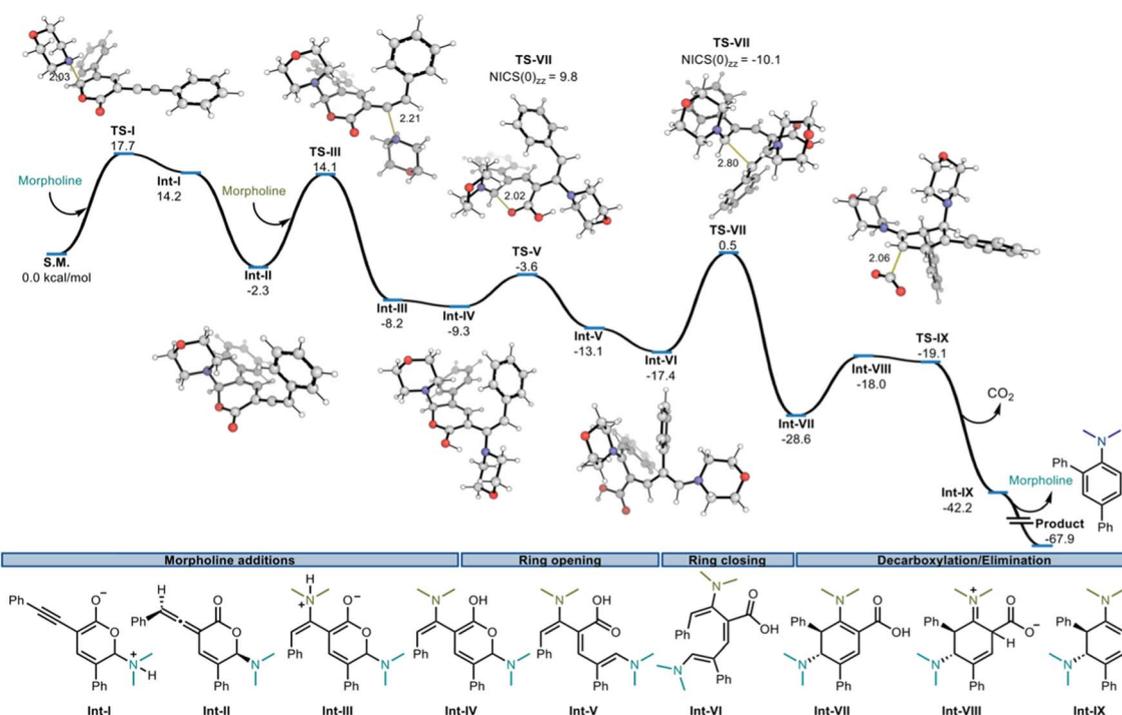

Fig. 1   Computed Gibbs free energy profile at 296.15 K, 1 M standard state at the SMD ωB97X-D/def2-TZVP//ωB97X-D/6-31+G(d,p) level of theory. Morpholine structure abbreviated for clarity.

to **Int-III** ($\Delta G = -5.9$ kcal mol^{-1}). Competing attack on the other face of the allene, which would lead to the Z alkene, was found to be higher in energy (**TS-III-Z**, 17.7 kcal mol^{-1}). Intramolecular proton transfer at this point yields **Int-IV**, which then undergoes extremely facile ring opening ($\Delta G^{\ddagger} = 5.7$ kcal mol^{-1}, **TS-V**) to produce triene **Int-V** ($\Delta G = -3.8$ kcal mol^{-1}).

Isomerization of the central double bond in E,Z,Z-configured triene **Int-V** to E,E,Z-configured **Int-VI** is thermodynamically favorable ($\Delta G = -4.3$ kcal mol^{-1}) and facilitates electrocyclic ring-closure ($\Delta G^{\ddagger} = 18.0$ kcal mol^{-1} *via* **TS-VII**), to give cyclohexadiene **Int-VII** in exergonic fashion ($\Delta G = -11.2$ kcal mol^{-1}). Ring closure from an E,E,E-configuration has a higher computed barrier (19.9 kcal mol; see **TS-VII-TRANS**, Fig. S6†). The subsequent steps involve decarboxylation *via* **TS-IX** (barrier of 9.5 kcal mol^{-1}) and then elimination/rearomatization. We envisioned an acid promoted E1 pathway for this elimination step; N-protonation results in spontaneous departure of the amine during geometry optimizations. This process is exergonic by 25.7 kcal mol^{-1} to give the final product at -67.9 kcal mol^{-1} relative to starting materials. Overall, we obtained a Gibbs energy profile in which each step is kinetically feasible at the reaction temperature, and also exergonic. The largest activation barriers on this computed PES are associated with the initial nucleophilic addition of morpholine at C6 (**TS-I**, 17.7 kcal mol^{-1}), and with the ring-closure (**TS-VII**, 17.9 kcal mol^{-1}) step. [33] Additionally, the activation barrier for ring closing (TS-VII) is sensitive to steric bulk, and the barriers for ring closing show good correlation with reaction yields and our linear regression model.[34]

Furthermore, we investigated the electronic structure of the ring opening (*via* **TS-V**) and ring closing steps (*via* **TS-VII**) using Nucleus Independent Chemical Shift (NICS)[30] calculations. **TS-V** has a NICS$(0)_{zz}$ value of 9.8 ppm, the absence of ring current indicative of a polar process, consistent with the small barrier associated with this step. In contrast, **TS-VII** has a NICS$(0)_{zz}$ value of -10.1 ppm, the result of diamagnetic shielding from a circulating aromatic ring current in this TS, consistent with a pericyclic 6π-electrocyclic ring closure.

Conclusion

In conclusion, we have developed a novel method for the conversion of 3-alkynyl-2-pyrones to aniline derivatives under mild conditions. A proposed reaction mechanism involving 2 equivalents of a secondary amine coupling partner is supported by DFT calculations. Additionally, a robust linear regression model based on steric bulk to predict the reactivity of the amine coupling partner was demonstrated. This mild transformation serves as a complement to traditional Buchwald–Hartwig amination and other metal-catalyzed C(sp^2)–X amination reactions and expands the scope of ring systems that can be accessed from 2-pyrones.

Data availability

All the primary data for this article is included in the ESI.†

Author contributions

K. E. G. and R. S. made the original discovery, conceived the project, and formulated the initial mechanistic hypotheses. K. E. G. and J. T. performed all experimental work under the guidance of R. S. Amine featurization and modelling was performed by M. A. H. under the guidance of M. S. S. Transition state calculations and computational mechanistic studies were performed by L. L. under the guidance of R. S. P. K. E. G., M. A. H., L. L, and R. S. wrote the manuscript with input from M. S. S. and R. S. P.

Conflicts of interest

There are no conflicts to declare.

Acknowledgements

References

1 C. R. Jamison and L. E. Overman, Fragment Coupling with Tertiary Radicals Generated by Visible-Light Photocatalysis, *Acc. Chem. Res.*, 2016, **49**, 1578–1586.

2 M. Tomanik, I. T. Hsu and S. B. Herzon, Fragment Coupling Reactions in Total Synthesis That Form Carbon–Carbon Bonds via Carbanionic or Free Radical Intermediates, *Angew. Chem., Int. Ed.*, 2021, **60**, 1116–1150.

3 J. Pérez Sestelo and L. A. Sarandeses, Advances in Cross-Coupling Reactions, *Molecules*, 2020, **25**, 4500.

4 A. Biffis, P. Centomo, A. Del Zotto and M. Zecca, Pd Metal Catalysts for Cross-Couplings and Related Reactions in the

21st Century: A Critical Review, *Chem. Rev.*, 2018, **118**, 2249–2295.

5 P. Devendar, R.-Y. Qu, W.-M. Kang, B. He and G.-F. Yang, Palladium-Catalyzed Cross-Coupling Reactions: A Powerful Tool for the Synthesis of Agrochemicals, *J. Agric. Food Chem.*, 2018, **66**, 8914–8934.

6 D. A. Horton, G. T. Bourne and M. L. Smythe, The Combinatorial Synthesis of Bicyclic Privileged Structures or Privileged Substructures, *Chem. Rev.*, 2003, **103**, 893–930.

7 E. Vitaku, D. T. Smith and J. T. Njardarson, Analysis of the Structural Diversity, Substitution Patterns, and Frequency of Nitrogen Heterocycles among U.S. FDA Approved Pharmaceuticals: Miniperspective, *J. Med. Chem.*, 2014, **57**, 10257–10274.

8 Z. Zhang, X. He, G. Wu, C. Liu, C. Lu, Q. Gu, Q. Che, T. Zhu, G. Zhang and D. Li, Aniline-Tetramic Acids from the Deep-Sea-Derived Fungus *Cladosporium sphaerospermum* L3P3 Cultured with the HDAC Inhibitor SAHA, *J. Nat. Prod.*, 2018, **81**, 1651–1657.

9 T. U. H. Baumeister, M. Staudinger, M. Wirgenings and G. Pohnert, Halogenated anilines as novel natural products from a marine biofilm forming microalga, *Chem. Commun.*, 2019, **55**, 11948–11951.

10 R. Lygaitis, V. Getautis and J. V. Grazulevicius, Hole-transporting hydrazones, *Chem. Soc. Rev.*, 2008, **37**, 770.

11 Z. Ning and H. Tian, Triarylamine: a promising core unit for efficient photovoltaic materials, *Chem. Commun.*, 2009, 5483.

12 R. Eelkema and H. L. Anderson, Synthesis of End-Functionalized Polyanilines, *Macromolecules*, 2008, **41**, 9930–9933.

13 R. Dorel, C. P. Grugel and A. M. Haydl, The Buchwald–Hartwig Amination After 25 Years, *Angew. Chem., Int. Ed.*, 2019, **58**, 17118–17129.

14 S. D. Roughley and A. M. Jordan, The Medicinal Chemist's Toolbox: An Analysis of Reactions Used in the Pursuit of Drug Candidates, *J. Med. Chem.*, 2011, **54**, 3451–3479.

15 D. Dobler, M. Leitner, N. Moor and O. Reiser, 2-Pyrone – A Privileged Heterocycle and Widespread Motif in Nature, *Eur. J. Org Chem.*, 2021, **2021**, 6180–6205.

16 Q. Cai, The [4 + 2] Cycloaddition of 2-Pyrone in Total Synthesis, *Chin. J. Chem.*, 2019, **37**, 946–976.

17 S. C. Coote, 4-π-Photocyclization: Scope and Synthetic Applications, *Eur. J. Org Chem.*, 2020, **2020**, 1405–1423.

18 V. Palani, C. L. Hugelshofer and R. Sarpong, A Unified Strategy for the Enantiospecific Total Synthesis of Delavatine A and Formal Synthesis of Incarviatone A, *J. Am. Chem. Soc.*, 2019, **141**, 14421–14432.

19 V. Palani, C. L. Hugelshofer, I. Kevlishvili, P. Liu and R. Sarpong, A Short Synthesis of Delavatine A Unveils New Insights into Site-Selective Cross-Coupling of 3,5-Dibromo-2-pyrone, *J. Am. Chem. Soc.*, 2019, **141**, 2652–2660.

20 V. Palani, M. A. Perea, K. E. Gardner and R. Sarpong, A pyrone remodeling strategy to access diverse heterocycles: application to the synthesis of fascaplysin natural products, *Chem. Sci.*, 2021, **12**, 1528–1534.

21 K. E. Gardner and R. Sarpong, Synthesis of substituted benzoates using a rhodium-mediated Hopf cyclization of 1,3-dien-5-ynes accessed from 2-pyrones, *Tetrahedron Lett.*, 2023, **114**, 154272.

22 J. Bariwal and E. Van Der Eycken, C–N bond forming cross-coupling reactions: an overview, *Chem. Soc. Rev.*, 2013, **42**, 9283.

23 I. P. Beletskaya and A. D. Averin, Metal-catalyzed reactions for the C(sp²)–N bond formation: achievements of recent years, *Russ. Chem. Rev.*, 2021, **90**, 1359–1396.

24 S. Bhunia, G. G. Pawar, S. V. Kumar, Y. Jiang and D. Ma, Selected Copper-Based Reactions for C–N, C–O, C–S, and C–C Bond Formation, *Angew. Chem., Int. Ed.*, 2017, **56**, 16136–16179.

25 M. Fitzner, G. Wuitschik, R. J. Koller, J.-M. Adam, T. Schindler and J.-L. Reymond, What can reaction databases teach us about Buchwald–Hartwig cross-couplings?, *Chem. Sci.*, 2020, **11**, 13085–13093.

26 M. M. Heravi, V. Zadsirjan, M. Malmir and L. Mohammadi, Buchwald–Hartwig reaction: an update, *Monatsh. Chem.*, 2021, **152**, 1127–1171.

27 K.-M. Ryu, A. K. Gupta, J. W. Han, C. H. Oh and C.-G. Cho, Regiocontrolled Suzuki-Miyaura Couplings of 3,5-Dibromo-2-pyrone, *Synlett*, 2004, **2004**, 2197–2199.

28 J.-H. Lee, J.-S. Park and C.-G. Cho, Regioselective Synthesis of 3-Alkynyl-5-bromo-2-pyrones via Pd-Catalyzed Couplings on 3,5-Dibromo-2-pyrone, *Org. Lett.*, 2002, **4**, 1171–1173.

29 For substrates where the desired product was isolated in low yield, we mostly observed unreacted starting material.

30 W. A. Henderson and C. J. Schultz, The Nucleophilicity of Amines, *J. Org. Chem.*, 1962, **27**, 4643–4646.

31 P. Raghavan, B. C. Haas, M. E. Ruos, J. Schleinitz, A. G. Doyle, S. E. Reisman, M. S. Sigman and C. W. Coley, Dataset Design for Building Models of Chemical Reactivity, *ACS Cent. Sci.*, 2023, **9**, 2196–2204.

32 S. H. Newman-Stonebraker, S. R. Smith, J. E. Borowski, E. Peters, T. Gensch, H. C. Johnson, M. S. Sigman and A. G. Doyle, Univariate classification of phosphine ligation state and reactivity in cross-coupling catalysis, *Science*, 2021, **374**, 301–308.

33 We also explored two alternative sequences of reactions from **Int-V** to the product (Fig. S6†). Firstly, decarboxylation before ring closing via **TS-VI-A** and then **TS-VIII-C**, has an associated activation barrier of 20.9 kcal mol⁻¹. On the other hand, ring closing followed by elimination before decarboxylation (*via* **TS-X-ZwitterionC**) had an associated barrier of 28.9 kcal mol⁻¹. Both of these processes are higher in energy relative to the favored mechanism but might account for potentially competing pathways that lead to the product.

34 For a detailed discussion of how the identity of the amine affects the activation barriers for **TS-I** and **TS-VII**, see the ESI.†